IOP Conf. Series: Materials Science and Engineering **117** (2016) 012016 doi:10.1088/1757-899X/117/1/012016

A simple model for spherical growth in alloy solidification

Z Fan[a] and S Z Lu
BCAST, Brunel University London, Uxbridge, Middlesex, UB8 3PH, UK.

Email: [a]Zhongyun.fan@brunel.ac.uk

Abstract. During alloy solidification, spherical growth is the initial growth stage immediately after heterogeneous nucleation but before the morphological instability for dendritic growth. A number of analytical solutions are available for spherical growth and Zener's approximation has been used in nearly all such models. These models, however, are only applicable to solidification with very small supersaturation. In this paper, based on the theoretical analysis of precipitation growth in solid state we present a simplified analytical expression for spherical growth applicable to solidification with an entire range of supersaturation.

1. Introduction

Crystal growth during alloy solidification has two distinctive stages, spherical growth and dendritic growth [1]. When a liquid alloy is cooled down to a temperature below its liquidus to reach the required undercooling for heterogeneous nucleation tiny crystals are nucleated. The initial growth after nucleation is spherical and this is followed by dendritic growth after morphological instabilities take place.

Spherical growth keeps a minimum ratio of interface area to the sphere volume so it is stable at the beginning. The Gibbs-Thomson effect due to curvature is the main driving force for growth when the sphere is very small. The solid crystal grows in spherical shape while continuously rejecting solute to the liquid ahead of the solidification front. As a result, the growing sphere is gradually surrounded by a solute rich layer [1]. With the increase of the sphere size, more and more solute is accumulated at the growth front and the curvature effect is getting less while solute will have more and more effect on growth. The solute rich layer in the liquid restricts the growth and becomes a destabilizing factor for the growth. The sphere particle grows in a balance between the stabilizing factor from the curvature and the destabilizing factor from the solute accumulated at the solid-liquid interface until the solute effect dominates the growth and interface instability occurs [2]. A transition from spherical growth to dendritic growth will then occur to accommodate the interface instability and surface energy anisotropy [3].

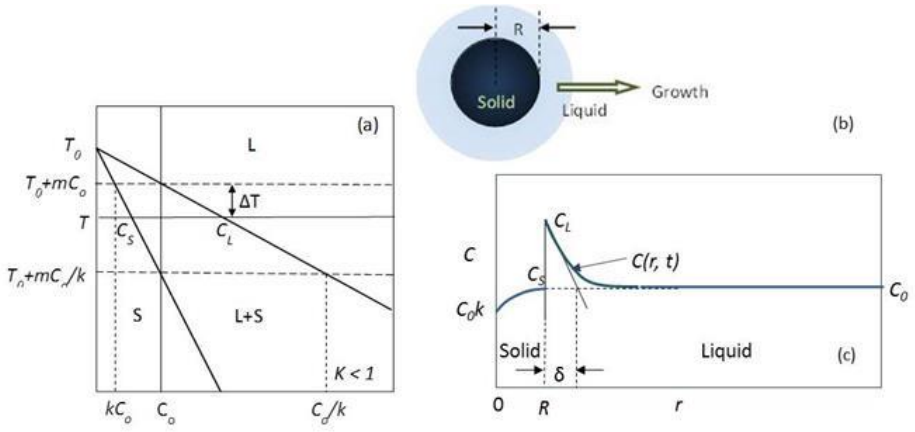

Figure 1. (a) A typical phase diagram with single phase solidification for an alloy of composition, C0, with the equilibrium solute partition coefficient, k, freezing range, ΔT_0, and the undercooling, ΔT. (b) Schematic representation of spherical growth model with the radius, R; a solute-rich liquid layer is around the solid sphere; (c) composition profile at the growth front. δ is defined as the characteristic diffusion length.

Figure 1 (a) shows a part of a typical phase diagram for single phase solidification of an alloy with composition C_0 for the case of equilibrium partition coefficient, k < 1. The solidification with spherical growth occurs in a spatially isothermal melt at a temperature T with an undercooling, ΔT, as indicated in figure 1 (a). Assume that there is no convection in the liquid and there is no interaction between solid spheres during solidification, the growth is completely controlled by diffusion and local equilibrium is then always maintained at the solid-liquid interface. As illustrated in figure 1 (b), r is the radial distance and R is the radius of the solid sphere. The solute profile in the liquid at the growth front is schematically represented in figure 1 (c). The compositions at the interface for the solid and the liquid are C_S and C_L, respectively. The growth rate depends on how fast the solute diffuses away from the interface to the bulk liquid.

Because the spherical growth is the very early stage of crystal growth with a short time duration, there has been so far very little research effort on spherical growth and the majority of the effort has been focused on dendritic growth [1, 4-9]. Zener, in his classical paper [10], provided an analysis for diffusion controlled solid state transformation in spherical form. This analysis is referred as "Zener Approximation" and has been used to treat the spherical growth in solidification [1, 10-13]. In Zener Approximation, the characteristic diffusion length is taken the same as the particle radius, R, and a linear concentration profile is assumed. This resulted in a simple expression for the velocity of spherical growth (V)

$$V = \alpha \frac{D_L}{R} \tag{1}$$

and

$$\alpha = \frac{C_L - C_0}{C_L - C_S} \tag{2}$$

where α is the solute supersaturation defined by Zener [10, 11]. Equation (1) has been used in models for grain size prediction [12, 13] because of its simplicity. In equation (1) the interface velocity is a sole linear function of α, solute supersaturation, for a given alloy. However, this expression can only be used when $\alpha << 1$ because the growth velocity calculated by equation (1) is contradictory to the classical theory of diffusion controlled growth, in which interface velocity becomes infinity as α goes to unity [11]. This is also equivalent to the steady state growth as $\Delta T \rightarrow \Delta T_0$ where ΔT_0 is the freezing range as shown in figure 1 (a).

In general, the interface velocity, *V*, is defined as

$$V = \frac{dR}{dt} = \frac{1}{2}\lambda\sqrt{\frac{D_L}{t}} = \frac{1}{2}\lambda^2\frac{D_L}{R} \tag{3}$$

where λ is a dimensionless interface parameter, $\lambda = \frac{R}{\sqrt{D_L t}}$, R is the radius of the solid sphere, D_L is the solute diffusion coefficient in liquid and is assumed to be constant, and t is the time. $\lambda^2/2$ is treated as the growth coefficient for a given size of sphere.

Maxwell and Hellawell [14] have used a simple spherical growth model to study grain refinement and revealed that not all the potent inoculants would trigger heterogeneous nucleation because of the recalescence. They followed the treatment by Aaron et. al. [15] for the diffusion controlled growth in solid state and developed an expression for spherical growth in their solidification model [14].

$$\lambda = \frac{\alpha}{\sqrt{\pi}} + \sqrt{\frac{\alpha^2}{\pi} + 2\alpha} \tag{4}$$

Figure 2 is a plot of $\lambda^2/2$ against the supersaturation, α, for both Zener approximation ($\lambda^2/2=\alpha$ in equation 1) and the Maxwell and Hellawell's model (equation 4). It can be seen that neither of the two equations above satisfies the classical theory of diffusion limited growth, in which interface velocity should reach infinity as α→1. As will be discussed later both Zener approximation and Maxwell and Hellawell's model are only accurate when α→0, they will not be applicable to solidification with large supersaturation.

In this paper we present an exact analytical solution and a simplified analytical expression for spherical growth applicable to solidification with entire range of supersaturation.

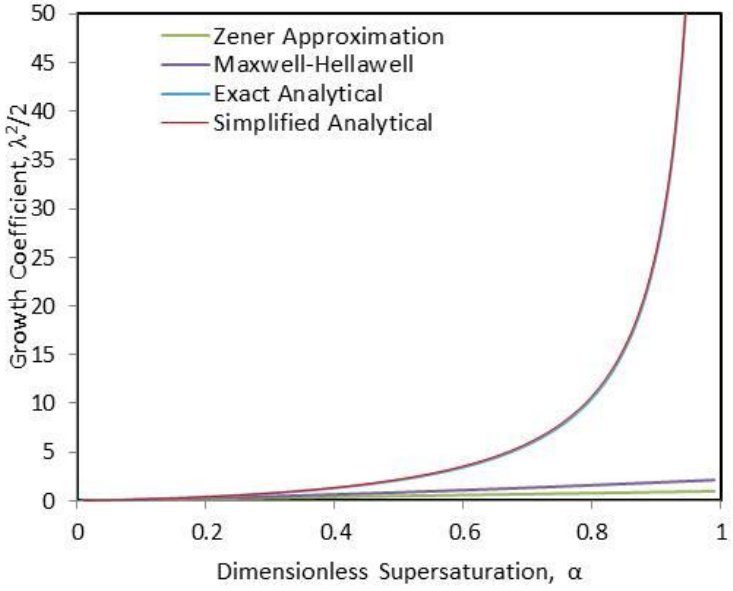

Figure 2. Plot of the Growth coefficient $\lambda^2/2$, against Dimensionless Supersaturation, α, for equation (1) of the approximate expression with Zener Approximation, where $\lambda^2/2 = \alpha$, equation (4) of the Maxwell-Hellawell expression, equation (14) of the analytical solution and equation (17) of the simplified expression.

2. A simple model

Consider the growth of a single solid sphere which does not interact with other spheres in an isothermal melt at temperature *T* (see figure 1), the sphere size is time dependent, $R=R(t)$ and $r=R$ is the solid-liquid interface position. The concentration profile at the S/L interface is a function of the

radial distance, *r*, and time, *t*, *C*=*C*(*r*,*t*). The governing equation for the diffusion controlled spherical growth is the Fick's second law:

$$\frac{\partial \mathrm{C}}{\partial \mathrm{t}} = \mathrm{D_L}[\frac{\partial^2 \mathrm{C}}{\partial \mathrm{r}^2} + \frac{2}{\mathrm{r}}\left(\frac{\partial \mathrm{C}}{\partial \mathrm{r}}\right)] \tag{5}$$

Equation (5) has the following initial and boundary conditions:

$$C(r \geq R, t = 0) = C_0 \quad C(r < R, t \geq 0) = C_s$$

$$C(r = R, t > 0) = C_L \quad C(r \to \infty, t > 0) = C_0$$

It has also to satisfy the mass balance at the solid-liquid interface described by the following equation:

$$\mathrm{V}(\mathrm{C_L} - \mathrm{C_S}) = -\mathrm{D_L}\left(\frac{\partial \mathrm{C}}{\partial \mathrm{r}}\right)_{\mathrm{r=R}} \tag{6}$$

The analytical solution is actually the same as given for solid state precipitation in [16] and [17] because it is the same in terms of diffusion theory:

$$\frac{\lambda^2}{2}\left[1 - \frac{1}{2}\sqrt{\pi}\lambda \exp\left(\frac{\lambda^2}{4}\right)\mathrm{erfc}\left(\frac{\lambda}{2}\right)\right] = \alpha \tag{7}$$

Equation (7) shows that the growth coefficient, $\lambda^2/2$, is an implicit function of solute supersaturation, α. For a given supersaturation, a unique value of growth coefficient can be numerically obtained and, consequently, the growth velocity can be calculated using equation (3). The numerically calculated growth coefficient from equation (7) is plotted in figure 2 as a function of solute supersaturation in the same way as the Zener approximation and the Maxwell-Hellawell expression above. It is clear in figure 2 that based on present analytical solution (equation 14) the growth coefficient $\lambda^2/2$ becomes very large when the supersaturation is approaching 1, which is consistent with the prediction by the classical diffusion controlled theory [11]. Neither the Zener approximation nor the Maxwell and Hellawell solution offer correct prediction when $\alpha \to 1$. Therefore, equations (1) and (4) can only be applied when $\alpha \to 0$. This is equivalent to the condition with a very small undercooling. When the solute undercooling is very large approaching the freezing range the results from equations (1) and (4) will deviate further from the exact analytical solution. It is also the case for very dilute alloys in which the freezing range is very small so that any small undercooling may result in a large supersaturation.

It should be pointed out that although the current analytical solution is derived for the case of $k < 1$, it is equally applicable to the cases of $k > 1$.

During solidification the growing solid sphere is surrounded by a solute rich liquid layer that is characterized by the characteristic diffusion lengths, δ (see figure 1 (c)). In diffusion controlled growth the growth velocity of the solid particle depends on how fast the solute accumulated in the layer can diffuse away from the solid/liquid interface to the bulk liquid. In other words, the solute accumulated at the interface will restrict crystal growth. It is expected that the thinner the solute boundary layer, the faster the growth. It is shown in figure 1 that the characteristic diffusion length is defined as:

$$\delta = \frac{\mathrm{C_0 - C_L}}{\left(\frac{\partial \mathrm{C}}{\partial \mathrm{r}}\right)_{\mathrm{r=R}}} \tag{8}$$

where $\left(\frac{\partial C}{\partial r}\right)_{r=R}$ is the concentration gradient in the liquid at the solid/liquid interface.

Following the same treatment as the diffusion controlled solid-solid transformation [17] the ratio of the characteristic diffusion length to the sphere size, δ/R is thus

$$\frac{\delta}{R} = \frac{2\alpha}{\lambda^2} \tag{9}$$

The δ/R ratio is a sole function of supersaturation since λ is also α dependent. A plot of the δ/R ratio against the supersaturation, α, is presented in figure 3. It is learned from figure 3 that the maximum ratio is when α approaches zero when the diffusion characteristic length, δ, is close to the sphere radius, R. This is the same as the Zener approximation for solid state transformation. It is then evident that the Zener approximation can only be accurate when α is close to zero. As the value of α is getting larger and larger the δ/R ratio is getting smaller and smaller until it goes to zero when α approaches one. This also suggests that the growth restriction at the growth front due to solute pile-up becomes smaller and smaller as the supersaturation is getting larger and larger and there is no growth restriction as the supersaturation reaches unity.

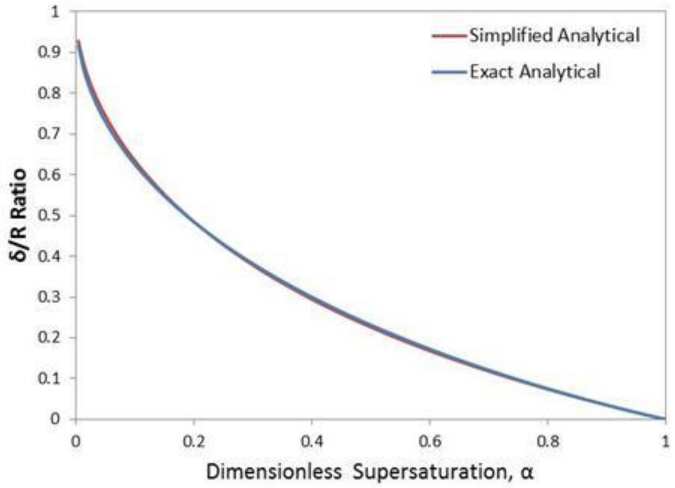

Figure 3. Plot of δ/R ratio against solute supersaturation, α, for both analytical solution and simplified analytical expression in which δ is the characteristic diffusion length and R is the radius of growing solid sphere.

The present model provides an accurate solution for diffusion controlled spherical growth during alloy solidification. As described in equation (3) and equation (7), the growth velocity is solely α dependent. However, the equation (7) is implicit and inconvenient to use. Therefore, there is a need to find a function of α that is a good fit of the exact solution over the entire range of α. Zener used asymptotic expansion to show that $\lambda^2/2 = \alpha$ as α goes to zero and $\frac{\lambda^2}{2} = \frac{3}{1-\alpha}$ approaches infinity as α goes to unity [10]. Through curve fitting for equation (7) and taking account of $\frac{\alpha}{1-\alpha} = \frac{C_0 - C_L}{C_S - C_0}$, a simplified analytical expression which satisfies asymptotic limits is obtained.

$$\frac{\lambda^2}{2} = \frac{\alpha}{1-\alpha}(1 + \sqrt{\alpha} + \alpha) \tag{10}$$

This simplified analytical expression, equation (10), is plotted together with the exact solution, i.e., equation (7), in figure 2. The two curves are almost overlapping over the whole range of the plot. Error analysis shows that the deviation of the simplified analytical expression from the exact analytical solution is less than 2% at the most from α=0.01 to 0.97. Therefore equation (10) can be a good replacement for equation (7) and it is much more convenient for practical application. Using the same replacement, the equation (9) for the normalized diffusion characteristic length can thus be presented as:

$$\frac{\delta}{R} = \frac{1-\alpha}{1+\sqrt{\alpha}+\alpha} \tag{11}$$

Equation (11) is also plotted in figure 3 in comparison with the analytical solution of equations (9). The two curves are again almost perfectly overlapping in whole range of α.

3. Discussion

As mentioned earlier, the Zener approximation can be used only when the supersaturation, α, is very small and this is the case when undercooling is small compared with the freezing range. For a very dilute alloy, the freezing range can be very small, it will be very easy to reach high supersaturation, and therefore, the approximate expressions, equations (1) and (3), can no longer be used. However, the present analytical model can provide an exact solution to such problems. Consider that two alloy melts are cooled below their respective liquidus but with the same undercooling (e.g., $\Delta T=0.25K$) which allows heterogeneous nucleation to occur. One alloy has a relatively large freezing range, Al-3 wt. % Cu (all compositions are in wt.% unless stated otherwise), for example; the other is a dilute alloy, e.g., Al-0.01 Ti. Due to the large difference in freezing range, the supersaturation will be different: α=0.04 for Al-3 wt. % Cu alloy and $\alpha=0.45$ for Al-0.01 Ti alloy. It is not a problem to use the approximate solutions for Al-3 Cu alloy, but there will be a large error for Al-0.01 Ti alloy. These data in comparison are listed in table 1. The growth velocities calculated with the approximate solutions and with present analytical solution are very close for Al-3 Cu alloy (a factor of 1.3) but will be very different for Al-0.01 Ti alloy (a factor of 4, see table 1).

Table 1. Data comparison for two alloy systems of Al – 3 wt.% Cu and Al – 0.01 wt.% Ti including Equilibrium Solute Partition Coefficient, k; Liquidus Slope, m; Freezing Range, $\Delta T_0=mC_0(k-1)$; Dimensionless Undercooling, $\theta=\Delta T/\Delta T_0$; Dimensionless Supersaturation, α; ratio of Characteristic Diffusion Length to Sphere Radius, δ/R; Growth coefficient, $\lambda^2/2$; and the ratio of the Interface Growth Velocities calculated by Analytical Solution to that calculated by the Approximate Solution. $\Delta T = 0.25\ K$ is assumed for both alloy systems.

					$\Delta T = 0.25\ K$				
	C_0 (wt.%)	k	m (K/wt.%)	ΔT_0 (K)	θ	α	δ/R	$\lambda^2/2$	Growth Velocity Ratio (Anal./ Appr.)
Al-Cu	3	0.14 [7]	-2.6 [7]	48	0.005	0.04 (α→0)	0.774	0.052	1.3
Al-Ti	0.01	7.67 [18]	33.3 [18]	0.3	0.83	0.45 (α>>0)	0.259	1.735	3.85

On the other hand, in the above cases with the same value of undercooling but different supersaturation in the two alloy systems, the characteristic diffusion lengths of the solute rich boundary layers are different for the same size of the particle since the ratios of δ/R is different. The calculated results using expression (11) shows that δ/R is 0.774 for Al-3 Cu alloy and 0.259 for Al-0.01 Ti alloy. This means that with the same undercooling ($\Delta T=0.25K$) the characteristic diffusion length for Al-3 Cu alloy is about three times thicker than that for the dilute Al-0.01 Ti alloy that has much higher supersaturation. It is conceivable that the growth will be more restricted with a thicker solute boundary layer at the solid/liquid interface, and consequently the growth rate will be slower. The calculated results of growth coefficient, $\lambda^2/2$, using equation (10) are indicators of the growth velocities that are consistent with the above understanding. These data are also listed in table 1 and they indicate that for the same solid particle size and undercooling, the growth velocity of dilute Al-0.01 Ti alloy is much higher than that of the Al-3 Cu alloy.

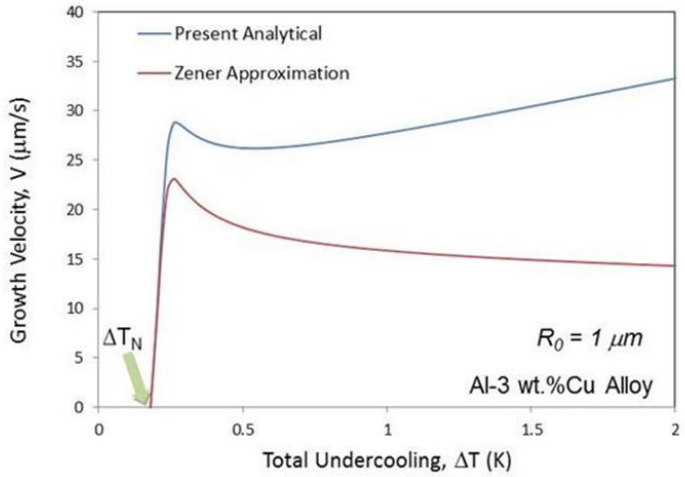

Figure 4. Plot of interface velocity against undercooling for Al- 3 wt. % Cu alloy calculated with the simplified analytical expression and with the approximate solution. ΔT_N is the initial undercooling after nucleation of the assumed solid sphere with radius R_0 = 1μm.

As described by equation (3), the velocity of spherical growth is proportional to the growth coefficient, $\lambda^2/2$, where $\lambda^2/2$ is a sole function of solute supersaturation, α, which in turn is a function of alloy composition, C_0, liquidus slope, m, and the solute partition coefficient, k. Considering the increasing radii during the spherical growth a plot of interface velocity against undercooling for Al- 3 Cu alloy is shown in figure 4. The undercooling is taken as the sum of the curvature term, $\Delta T_r = \frac{2\Gamma}{R}$ where $\Gamma = \frac{\sigma_{SL}}{\Delta S}$ is the Gibbs-Thomson coefficient, Γ=0.9 x 10^{-7} mK [7], and the solute term, $\Delta T_S = m(C_0 - C_L)$. The initial size of the sphere, R_0, after nucleation is assumed to be 1 μm in radius and the diffusion coefficient of copper in liquid aluminium, D_L = 3 x 10^{-9} m^2/s is taken in calculation [7]. The interface velocity calculated with the Zener approximation (equation 1) is also plotted in figure 4 for comparison. It is obvious that the Zener approximation does not give the correct trend that interface velocity goes up as the undercooling/supersaturation increases. The present model, on the other hand does give the right trend that velocity increases with the undercooling or supersaturation. As demonstrated above, the simplified expression is applicable to dilute alloys and can be used to examine the growth restriction effect of solute element during solidification.

4. Summary

Following the theoretical analysis of precipitation growth in solid state we have derived an exact solution for the growth of spheroids in liquid alloys, which describes the growth coefficient as an implicit function of the solute supersaturation. For convenience we have also converted the exact solution into a simplified analytical expression where the growth coefficient is an explicit function of the solute supersaturation. The present analytical solutions are applicable to spherical growth with the entire range of supersaturation ($0<\alpha<1$), and is a significant improvement over both the Zener approximation and the Maxwell and Hellawell's model in variant size approximation.

Acknowledgement

Professor J. D. Hunt had participated in this work before he passed away in 2012. The financial support from EPSRC (UK) under the grant for the EPSRC Centre-LiME is gratefully acknowledged.

References

[1] Dantzig J A and Rappaz M 2009 Solidification EPFL Press
[2] Mullins W W and Sekerka R F 1963 *Journal of Applied Physics* **34** 323
[3] Kessler D A Koplik J and Levine H 1988 *Advances in Physics* **37** 255
[4] Ivantsov G P Dokl 1947 *Akad. Nauk SSSR* **58** 567.
[5] Horvay G and Cahn J W 1961 *Acta Metall*. **9** 695
[6] Lipton J Glicksman M E and Kurz W 1984 *Materials Science and Engineering* **65** 57

[7] Kurz W and Fisher D J 1989 Fundamentals of Solidification, Lausanne: Trans. Tech.
[8] Trivedi R and Kurz W 1994 *International Materials Reviews* **39** 49
[9] Asta Beckermann M C Karma A Kurz W Napolitano R Plapp M Purdy G Rappaz M Trivedi R 2009 *Acta Materialia* **57** 941
[10] Zener C 1949 *Journal of Applied Physics* **20** 950
[11] Christian J W 1975 *The Theory of the Transformation of Metals*, Pergamon Press
[12] Wu M Ludwig A 2009 *Acta Materialia* **57** 5621
[13] Hunt J D and Fan Z 2011 Solidification Science and Technology, Proceeding of the John Hunt International Symposium, 12-14 December 2011, Brunel University Press 59
[14] Maxwell I and Hellawell A 1975 *Acta Metalurgica* **23** 229
[15] Aaron H B Fainstein D and Kotler G R 1970 *Journal of Applied Physics* **41** 4404
[16] Frank F C 1950 Proc. Roy. Soc. London **A201** 856
[17] Glicksman M E 2000 *Diffusion in Solids*, John Wiley & Sons, Inc.
[18] Desnain P Fautrelle Y Meyer J L Riquet J P Durand F 1990 *Acta Metall. Mater*. **38** 1513